

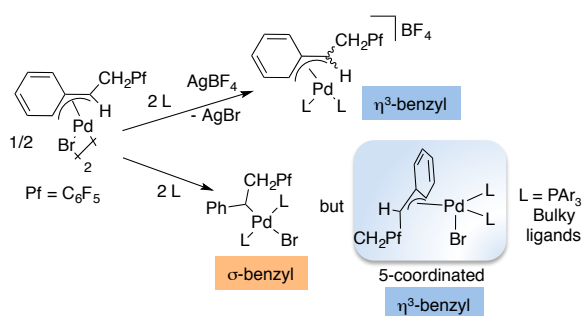
# Benzylic Complexes of Palladium(II): Bonding modes and Penta-coordination for Steric Relief.

Blanca Martín-Ruiz, Ignacio Pérez-Ortega and Ana C. Albéniz\*

IU CINQUIMA/Química Inorgánica. Universidad de Valladolid. E-47071 Valladolid. Spain.

Supporting Information

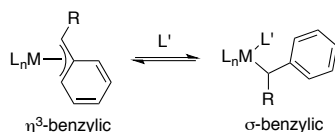
**ABSTRACT:** A large variety of  $\alpha$ -(pentafluorophenylmethyl)benzylic palladium complexes with different ligands have been synthesized and characterized. Multinuclear NMR spectroscopic data allow to determine the  $\sigma$ - or  $\eta^3$ -benzylic nature of the complexes in solution. The adoption of either coordination mode is a function of the number of ligands coordinated to palladium and, remarkably, the presence of bulky phosphines favors the adoption of a bidentate  $\eta^3$ -benzylic mode and palladium pentacoordinated complexes. Experimental data and DFT calculations indicate that this five-coordination could alleviate the steric hindrance of two cis bulky phosphines. The benzylic complexes show a rich fluxional behavior that involves both ligand exchange and  $\sigma$ - to  $\eta^3$ -benzylic interconversion.



## INTRODUCTION

Benzylic palladium complexes are frequently formed in Pd-catalyzed transformations of benzyl reagents and of styrene derivatives.<sup>1-6</sup> They can be considered weakly stabilized palladium alkyls by coordination of the aryl ring in a pseudoallylic ( $\eta^3$ ) form (Scheme 1). Yet, this  $\eta^3$ -interaction destroys the aromaticity of the ring and it is easily broken to return to the  $\sigma$ -benzylic form. In this way, benzylic metal derivatives show, in a more controlled way, the typical reactivity of metal alkyls. Also, by a shift from the bidentate  $\eta^3$ -benzylic to the monodentate  $\sigma$ -benzylic coordination mode an extra ligand can be accommodated, thus modifying the coordination sphere of the metal and influencing the dissociation-coordination processes that are important in any catalytic transformation (Scheme 1).

**Scheme 1.  $\sigma$ -benzylic and bidentate  $\eta^3$ -benzylic coordination modes.**



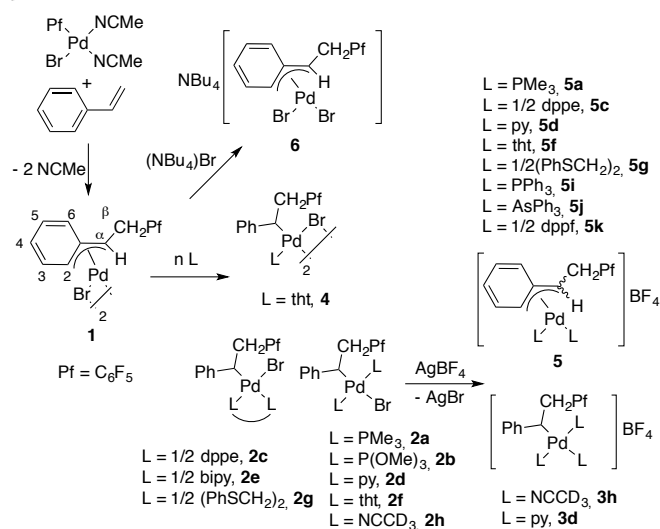
A rich variety of metal coordination environments, a priori difficult to anticipate, is possible for benzylic palladium complexes in combination with different ligands. It would be useful to gather some information regarding the type of coordination mode ( $\sigma$ - or  $\eta^3$ -benzylic) that can be expected and how it can be correlated to the nature of the other ligands bound to the metal. We describe

here a large family of palladium benzylic complexes with auxiliary ligands of different types and in different numbers, and analyze how they influence the type of benzylic coordination, the coordination number of the metal, and the fluxional behavior of the complexes.

## RESULTS AND DISCUSSION

Palladium(II) benzylic complexes bearing a pentafluorophenylmethyl substituent were prepared from complex **1** and are collected in Scheme 2. The dimeric complex **1** was synthesized by insertion of styrene into the Pd-C<sub>6</sub>F<sub>5</sub> bond of [PdBr(C<sub>6</sub>F<sub>5</sub>)(NCMe)<sub>2</sub>].<sup>7</sup> It precipitates in CH<sub>2</sub>Cl<sub>2</sub> so it can be easily isolated in good yield and it is a convenient starting material for the synthesis of other benzylic palladium derivatives. Upon addition of ligands to **1**, different coordination modes were found depending on the stoichiometric ratio [Pd]:ligand and the solvent used.  $\sigma$ - and  $\eta^3$ -(pentafluorophenylmethyl)benzyl complexes were generated and characterized in solution, and trends in the NMR data were found that allow to ascertain the coordination mode of the benzylic moiety. The presence of the pentafluorophenyl group is most useful since the simplicity and wide chemical shift range in its <sup>19</sup>F NMR spectra allow to detect new species and the composition of mixtures of isomers, if it is the case (see Figure S1 in the supporting information). Most complexes are fluxional and display a dynamic behavior that was evident in their NMR spectra and it is described below. The stability of the complexes is very different but all of them eventually decompose by  $\beta$ -H elimination. For this reason, many complexes were characterized at low temperature to guarantee enough stability and static spectra. In several cases the complexes were also isolated.

## Scheme 2. Benzylic palladium complexes from complex 1.



**$\sigma$ -Benzylic derivatives.** This type of complexes can be obtained by addition of two equivalents of a monodentate ligand per palladium or one equivalent of a bidentate ligand per Pd to complex **1** in a non-coordinating solvent, such as chloroform or dichloromethane (**2**, Scheme 2). Thus, both bridge cleavage and  $\eta^3$  to  $\sigma$  coordination change occur for most ligands. NMR data are collected in Tables 1, 2 and 4 ( $^1\text{H}$ ,  $^{13}\text{C}$  and  $^{31}\text{P}$ , see Experimental) and Table S1 ( $^{19}\text{F}$ , see Supporting Information).

All complexes show characteristic spectroscopic features of the  $\sigma$ -benzylic coordination mode. The salient feature is the chemical shift of  $\text{C}^\alpha$  in the  $^{13}\text{C}$  NMR spectra at about 30–44 ppm and  $^1\text{J}_{\text{C}^\alpha-\text{H}} = 130\text{--}140$  Hz, in the range of  $\text{C}(\text{sp}^3)\text{-H}$  coupling (Figure S4). The  $^1\text{H}$  NMR signals in the aromatic region generally follow the trend:  $\delta \text{H}_{\text{para}} < \delta \text{H}_{\text{meta}} < \delta \text{H}_{\text{ortho}}$  with equivalent ortho hydrogens or meta hydrogens in a freely rotating phenyl group.

The cis or trans stereochemistry of the complexes with monodentate ligands is unequivocally determined by  $^{31}\text{P}$  NMR for the phosphino derivatives and, when possible ( $L = \text{py}$ ), by the  $^1\text{H}$  NMR pattern of the ligand signals. Neither the cis nor the trans situation produces the equivalence of both L ligands, due to the chiral  $\text{C}^\alpha$  carbon. However, very close chemical shifts for the active nuclei of L are observed for the trans isomers, vs. well-separated signals for the cis isomers (Figure S2). Trans  $\sigma$ -benzylic complexes are obtained as the only product for  $L = \text{PMe}_3$  (**2a**) or the major species for  $L = \text{P(OMe)}_3$  (**2b**) and  $\text{py}$  (**2d**). In the latter cases the cis isomer is formed in a trans:cis ratio 7:1 for **2b** at 223 K in  $\text{CDCl}_3$ , and 3.3:1 for **2d** at 273 K in  $\text{CDCl}_3$ .<sup>8</sup> The stereochemistry of the complexes for  $L = \text{tht}$  (**2f**) and  $\text{NCMe}$  (**2h**) could not be unequivocally assigned, but by analogy to the preceding examples, we assume a trans geometry. The crystal structure of complex **2g** has been determined by X-ray diffraction and is shown in Figure 1 (a). The  $\sigma$ -coordination of the benzylic group can be observed along with the anti conformation of both phenyl rings in the bis(phenylthio)ethane ligand. The Pd-S distances are quite different and show the higher trans influence of the benzylic group when compared to the bromo ligand (Pd-S2 = 2.460 (4) Å vs. Pd-S1 = 2.334 (4) Å). Selected distances and angles are given in Table S3.

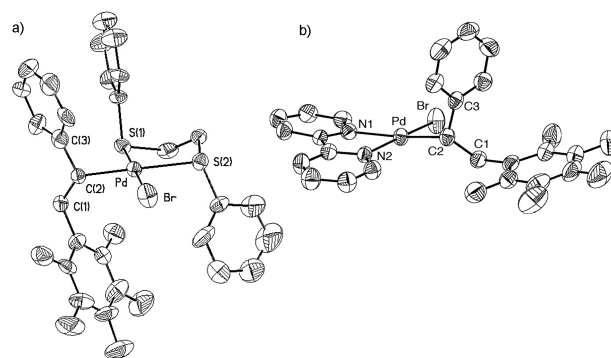
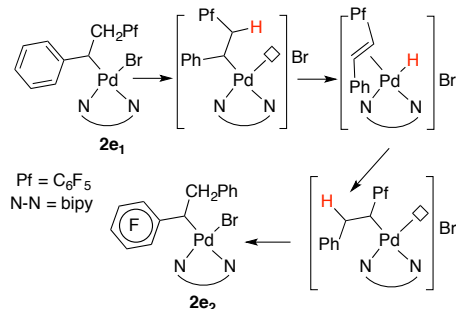


Figure 1. Molecular structures with complexes **2g** (a) and **2e1** (b). Selected distances (Å) for **2g**: Pd-C2 2.080(12), Pd-Br 2.475(2), Pd-S2 2.460(4), Pd-S1 2.334(4); **2e1**: Pd-C2 2.059(5), Pd-Br 2.4365(11), Pd-N1 2.153(4), Pd-N2 2.108(5).

The bipyridine complex (**2e**) is a mixture of two isomers in solution in a 5:1 ratio. Both show a typical ABX spin system for the  $\text{H}^\alpha$  and  $\text{H}^\beta$  protons of the benzylic group, but  $\text{H}^\alpha$  of the minor isomer (**2e2**) is clearly shifted downfield ( $\delta$  5.57 vs.  $\delta$  3.93 for the major isomer **2e1**). We attribute both isomers to the two  $\sigma$ -benzylic derivatives shown in Scheme 3, where **2e2** is formed by  $\beta$ -H elimination and readdition from **2e1**. The fluxional behavior of these complexes is consistent with the structures proposed as will be described below. Exchange between  $\text{H}^\alpha$  and  $\text{H}^\beta$  in cationic methylbenzyl derivatives of palladium has been observed before and occurs by the same  $\beta$ -H elimination-readdition pathway.<sup>9</sup> The crystal structure of the major isomer (**2e1**) has been determined (Figure 1, b) and significant distances and angles are collected in Table S4. A small deviation from square planar geometry is observed (the dihedral angle between the planes that contain Pd-Br-C2 and Pd-N1-N2 is  $9.1^\circ$ ),<sup>10</sup> and the  $\sigma\text{-CH}(\text{CH}_2\text{C}_6\text{F}_5)\text{Ph}$  group shows similar features than those of complex **2g**. When crystals of complex **2e1** are dissolved in  $\text{CDCl}_3$  at room temperature a mixture of both isomers **2e1** and **2e2** is observed, whereas only **2e1** is present if the crystals are dissolved at 253 K. This confirms that the minor isomer is generated from **2e1**.

## Scheme 3. Generation of the minor isomer **2e2** from **2e1**.



Complex **2h** is formed when a large excess of the weakly coordinating acetonitrile is present, i.e. when **1** is dissolved in  $\text{NCMe}$ . The chemical shift of  $\text{C}^\alpha$  (43.45 ppm) indicates a  $\sigma$ -coordination of the benzylic group. When the bromo ligand is eliminated by precipitation with a silver salt, the cationic complex **3h** also retains a  $\sigma$ -benzylic ligand (Scheme 2). The analogous **3d** was obtained upon addition of an excess of pyridine to a solution of **3h** in acetonitrile. In these cases, the electrophilic cationic metal

center coordinates an extra  $\sigma$ -donor ligand to complete its coordination sphere rather than adopting an  $\eta^3$ -benzylic coordination mode.

The type of complex formed upon addition of a monodentate ligand in a ratio Pd:L = 1:1 is more difficult to anticipate. As can be seen in Scheme 2, both  $\sigma$ - and  $\eta^3$ -benzylic coordination are possible (**4**, **6**). Complex **4** was formed upon addition of tetrahydrothiophene (tht) in a ratio Pd:tht = 1:1. Although the initial  $\eta^3$ -coordination in **1** does not need to be changed to accommodate the new ligand, the formation of a  $\sigma$ -benzylic dimeric derivative is preferred to a bridge cleavage. The chemical shift of C $^\alpha$ , 37.1 ppm, is characteristic of this arrangement. At 223 K, **4** is a mixture of two isomers derived from the relative cis and trans arrangement of the ligands in the dimer. These isomers undergo fast interconversion at temperatures above 283 K.<sup>11</sup>

**$\eta^3$ -Benzylic derivatives.** The elimination of the bromide in complexes **2a-g** by treatment with a silver salt leads to the cationic  $\eta^3$ -pentafluorobenzylbenzyl complexes **5a-g** (Scheme 2). NMR data for all  $\eta^3$ -benzylic complexes are collected in Tables 2, 3 and 4 (<sup>13</sup>C, <sup>1</sup>H and <sup>31</sup>P, see Experimental) and Table S1 (<sup>19</sup>F, see Supporting Information). The  $\eta^3$ -coordination mode is characterized spectroscopically by the chemical shift for the C $^\alpha$  in the <sup>13</sup>C NMR spectra around 60 ppm and a value of <sup>1</sup>J<sub>C $^\alpha$ -H</sub> close to 155 Hz consistent with an sp<sup>2</sup> carbon atom. Both parameters have higher values than those of the  $\sigma$ -benzylic situation and allow us to distinguish both coordination modes. Complexes with triaryl phosphines or AsPh<sub>3</sub> **5i-k**, **7** and **8** are also  $\eta^3$ -benzylic complexes but their behavior shows distinct features and they will be discussed separately.

In a static  $\eta^3$ -benzylic complex the ortho and meta protons of the phenyl ring are inequivalent and H<sup>2</sup> is clearly shifted upfield. The aromatic signals in the <sup>1</sup>H NMR spectra usually follow the trend:  $\delta$  H<sup>2</sup> <  $\delta$  H<sup>6</sup> <  $\delta$  H<sup>3</sup>, H<sup>5</sup> <  $\delta$  H<sup>4</sup>. However, a fast  $\eta^3$ - $\sigma$ - $\eta^3$  equilibrium can exchange H<sup>2</sup> and H<sup>6</sup> by rotation of the phenyl ring, leading to one signal for both protons, and this is observed for some of the complexes prepared (Figure S5).<sup>12</sup> Depending on the ligand this process can occur at very different rates. Table 3 collects the chemical shifts for H<sup>2</sup> and H<sup>6</sup> for the  $\eta^3$ -benzylic derivatives showing examples of quite a fast exchange (i.e. **5a** with the good donor PMe<sub>3</sub>, where equivalent signals are found at 223 K), a slow one (inequivalent signals at room temperature, i.e. **5d**) or show a temperature dependent behavior (complex **6**). As an example, the  $\eta^3$ -benzylic complex **1** shows a static <sup>1</sup>H NMR spectrum in CDCl<sub>3</sub> at room temperature (Figure 2). Upon addition of two equivalents of acetonitrile, the coalescence of the H<sup>2</sup> and H<sup>6</sup> signals is observed, which indicates a fast  $\eta^3$ - $\sigma$ - $\eta^3$  interconversion that allows, by rotation, the equivalence of both H<sub>ortho</sub> aromatic protons. The  $\eta^3$ - $\sigma$  equilibrium is altered when more acetonitrile is added and, as it was mentioned above, the  $\sigma$ -benzylic complex (**2h**) is the species present in solution when **1** is dissolved in MeCN.

Only one of the two possible isomers of the  $\eta^3$ -pseudoallylic coordinated benzyl group (syn and anti, Chart 1) is observed at any of the temperatures used for characterization for all the complexes prepared. A fast suprafacial sigmatropic rearrangement in solution can produce the transformation of the syn into the anti  $\eta^3$ -benzylic isomer,<sup>12a,13</sup> and it would lead to average spectra in the

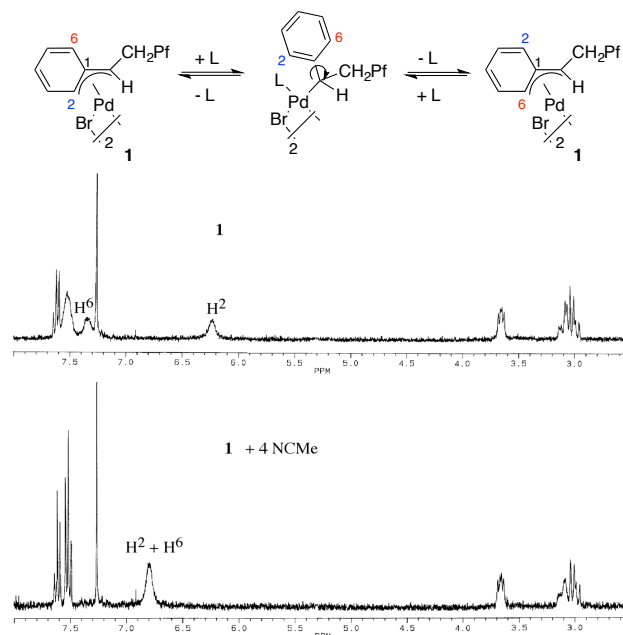
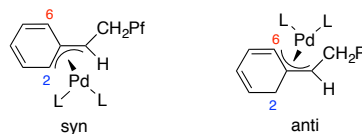


Figure 2.  $\eta^3$ - $\sigma$ - $\eta^3$  interconversion that results in the coalescence of H<sup>2</sup> and H<sup>6</sup> signals in the <sup>1</sup>H NMR spectra of complex **1** in CDCl<sub>3</sub> upon addition of NCMe.

H $^\alpha$  and H $^\beta$  region, which could be misinterpreted as the presence of only one species. The stability of both isomers as well as the chemical shift of H $^\alpha$  are expected to be different. Thus, in a fast exchange scenario the variation of the equilibrium constant upon changing the temperature should be reflected in a significant change in the chemical shifts of H $^\alpha$ , which is not observed in any of the complexes studied. In complex **1** the -CH<sub>2</sub>C<sub>6</sub>F<sub>5</sub> substituent is accommodated in the syn position, far from the metal center, and the presence of this isomer is confirmed by the NOE effect observed between H $^\alpha$  and H<sup>2</sup> in a <sup>1</sup>H 2D-ROESY experiment (Figure S8). This experiment was also carried out for complexes **5c** and **5f** but the results are less conclusive. In both cases, even at low temperature, the phase sensitive ROESY experiment shows slow H<sup>2</sup>-H<sup>6</sup> exchange. The same experiment shows a high intensity NOE cross-peak between H $^\alpha$  and H<sup>2</sup>, but a less intense NOE effect between H $^\alpha$  and H<sup>6</sup> is also present. A syn  $\eta^3$ -benzyl isomer where a slow shift to a  $\sigma$ -benzyl and aryl rotation rotation takes place as described above (Figure 2), explains the results obtained but does not rule out the sigmatropic shift (Chart 1).

#### Chart 1. Possible syn and anti isomers of the $\eta^3$ -benzylic moiety.

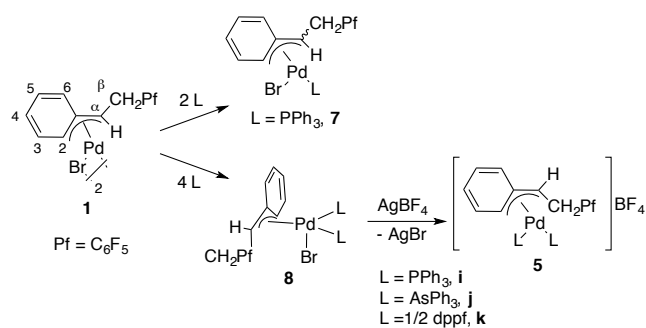


The addition of NBu<sub>4</sub>Br to complex **1** in a Pd:Br<sup>-</sup> = 1:1 ratio leads to a species that show broad signals in the <sup>19</sup>F and <sup>1</sup>H spectra. These are transformed into well resolved signals when and excess of bromide is added (Pd:Br = 1:5) pointing to an equilibrium between complexes **1** and **6**. Complex **6** is an  $\eta^3$ -benzylic derivative (C $^\alpha$ , 54.6, <sup>1</sup>J<sub>C $^\alpha$ -H</sub> = 154.7 Hz) with shows a static structure at 223 K but a fast H<sup>2</sup>-H<sup>6</sup> exchange at 293 K. The coordina-

tion of an additional bromide to give a  $\sigma$ -benzylic dianionic complex is not favored.

**$\eta^3$ -Benzylic complexes with L = PPh<sub>3</sub>, AsPh<sub>3</sub>, dppf: pentacoordinated derivatives.** The behavior of these ligands, the bulkiest we tried, is clearly different and shows surprising structures in solution to cope with the steric hindrance imposed by L. The addition of one equivalent of triphenylphosphine per palladium to complex **1** brings about the formation of the  $\eta^3$ -benzylic complex **7** (Scheme 4), as expected. A static <sup>1</sup>H NMR spectrum is observed at 213 K with separated signals for H<sup>2</sup> ( $\delta$  6.97) and H<sup>6</sup>. The cis arrangement of C <sup>$\alpha$</sup>  and PPh<sub>3</sub> is proposed according to the low value of <sup>3</sup>J<sub>P-H <sup>$\alpha$</sup>  (< 6 Hz) and <sup>2</sup>J<sub>P-C <sup>$\alpha$</sup>  (< 20 Hz). However, the behavior observed when 2 equivalents of PPh<sub>3</sub> per palladium are added to a CDCl<sub>3</sub> suspension of **1** at 213 K is different to the one described for other monodentate ligands. An  $\eta^3$ -benzylic complex (**8i**) is formed (C <sup>$\alpha$</sup> , 60.63 ppm; <sup>1</sup>J<sub>C <sup>$\alpha$</sup> -H = 155 Hz; H<sup>2</sup> and H<sup>6</sup>, 6.77 ppm), with two inequivalent phosphine ligands in a cis arrangement (<sup>2</sup>J<sub>P-P</sub> = 51.9 Hz). The bromo ligand is not out of the coordination sphere of palladium, since the addition of AgBF<sub>4</sub> leads to a different species, the cationic  $\eta^3$ -benzylic derivative **5i** (C <sup>$\alpha$</sup> , 70.5 ppm; <sup>1</sup>J<sub>C <sup>$\alpha$</sup> -H = 155 Hz; H<sup>2</sup>, 6.72 ppm; H<sup>6</sup>, 7.11 ppm; <sup>2</sup>J<sub>P-P</sub> = 47 Hz). Thus, complex **8i** must be the pentacoordinated species shown in Scheme 4 as a square pyramidal (spy), although trigonal bipyramidal (tbp) or distorted square pyramidal palladium species have been isolated, and either arrangement is consistent with our spectroscopic data.<sup>14-17</sup> The spy structure shown in Scheme 4 is proposed based on DFT calculations (see below), since the low stability of complex **8i** prevented its crystallization for X-ray diffraction structure determination. The same behavior was found for L = AsPh<sub>3</sub> (**8j**) and L = 1/2 diphenylphosphinoferrrocene (dppf, **8k**) and complete spectroscopic data for these complexes can be found in Tables 2-4 (see Experimental).</sub></sub></sub></sub>

**Scheme 4.  $\eta^3$ -benzylic complexes formed from **1** upon addition of aryl phosphines.**



Since complexes **8** are generated and characterized in a solvent of low polarity such as CDCl<sub>3</sub>, we hypothesized that they could form tight ionic pairs in solution, so the spectroscopic features of **8** and **5** would be a result of a different interaction between the cation and either bromide or BF<sub>4</sub><sup>-</sup>. We generated complex **8i** in acetone at 223 K and measured the conductivity of the solution at this temperature to find a nonelectrolyte. The  $\eta^3$ -benzylic mode (C <sup>$\alpha$</sup> , 52.37 ppm) and coordination sphere of palladium (two PPh<sub>3</sub> in a cis arrangement) are maintained in acetone, supporting the occurrence of a pentacoordinated species.

The cationic complexes **5i-k** show static <sup>1</sup>H NMR spectra below 223 K at 300 MHz, with anti configuration for the  $\eta^3$ -benzylic group supported by the observation in solution of NOE effect between H <sup>$\alpha$</sup>  and H<sup>6</sup> (cross peak in a <sup>1</sup>H 2D-ROESY experiment). A molecular structure of **5k** obtained using low quality crystals also shows the anti arrangement of the  $\eta^3$ -benzylic group (see Figure S13).<sup>18</sup> This is in contrast to complex **1** where the syn isomer was found, and to other  $\eta^3$ -benzylic complexes discussed before (**5c**, **5f**) where the syn isomer is also present (although maybe not exclusively, see the preceding section). It is also somewhat surprising, since the syn-arrangement in allylic compounds generally results in less steric hindrance. Density functional theory (DFT) calculations were carried out using the M06 functional for both syn and anti isomers of complex **5i** (L = PPh<sub>3</sub>) and also for both isomers of the dppe analogue complex **5c** (see computational details in the Experimental). Geometries were initially optimized with a medium-sized basis set (LANL2DZ ECP for Br and SDD for Pd and 6-31+G(d) for all other atoms), including solvation (SMD, dichloromethane as solvent). The resultant free energies were then corrected with an extended basis set (LANL2DZ ECP again for Br and SDD def2-QZVP for Pd but 6-311++G\*\* for all other atoms). As mentioned above <sup>1</sup>H 2D-ROESY experiments indicate that in solution **5i** adopts in solution the anti configuration whereas a stronger cross peak between H <sup>$\alpha$</sup>  and H<sup>2</sup> indicates that **5c** corresponds to the syn isomer (Figures S9-12). Both complexes are ionic and their optimized geometries were first calculated just considering the cation. However, since our experimental data were collected in dichloromethane, a low polarity, low dielectric constant solvent, the interaction with the tetrafluoroborate anion was also considered.<sup>19</sup> All the structures and the calculated energies are collected in the Supporting Information. Figure 3 shows the optimized structures of the syn and anti isomers for **5i** and **5c** and their relative energies, as well as selected geometrical parameters.

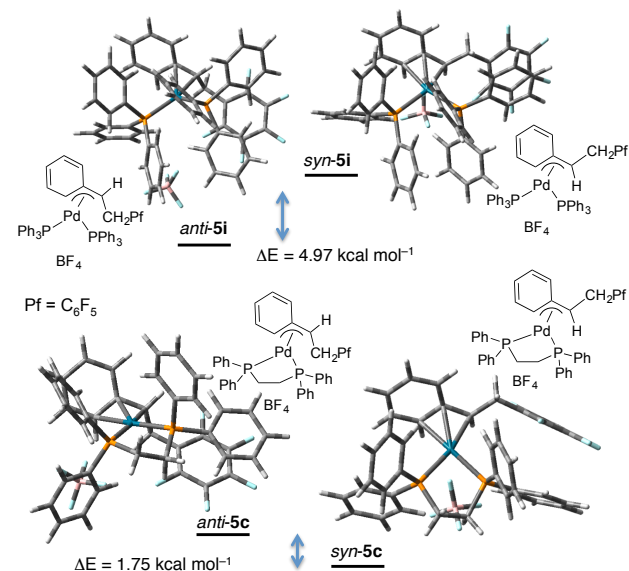


Figure 3. Optimized structures of the syn and anti isomers of **5i** and **5c** and their relative energies. Selected geometrical parameters: P-Pd-P = 103.78° (anti-**5i**); 100.66° (syn-**5i**); 83.76° (anti-**5c**); 84.59° (syn-**5c**); Pd-C <sup>$\alpha$</sup> , Pd-C2 (Å) = 2.123, 2.602 (anti-**5i**); 2.156, 2.426 (syn-**5i**); 2.143, 2.429 (anti-**5c**); 2.168, 2.348 (syn-**5c**).

There is a clear energy preference for the anti configuration in complex **5i** (4.97 kcal mol<sup>-1</sup>). This isomer shows a less symmetrical benzylic moiety (Pd-C<sup>α</sup>, Pd-C2 (Å): 2.123, 2.602 (anti-**5i**); 2.156, 2.426 (syn-**5i**)) and a wider P-Pd-P angle (P-Pd-P = 103.78° for anti-**5i** vs. 100.66° for syn-**5i**), which could help to accommodate the two sterically demanding cis-PPh<sub>3</sub>. In contrast, there is a very small energy difference for both isomers of **5c** and the syn isomer is slightly favored (1.75 kcal mol<sup>-1</sup>). This difference is very small but enough to observe just one isomer as a major species in solution ( $K = 5 \cdot 10^{-2}$ ). The geometrical parameters for both **5c** isomers are very similar. Given the lower steric demand of dppe and its lower bite angle, the adoption of an anti configuration, which allows a wider P-Pd-P angle as observed for **5i**, does not introduce any significant decrease in steric hindrance.

The distinct behavior of complexes **8i-k**, synthesized by addition of a twofold molar amount of PPh<sub>3</sub> or AsPh<sub>3</sub> per Pd or an equimolar amount of dppf, can be attributed to the steric features of these ligands rather than to electronic factors. Complexes **2a** and **2b**, with more (L = PMe<sub>3</sub>) or less (L = P(OMe)<sub>3</sub>) electron donating phosphines than PPh<sub>3</sub> are σ-benzylic four-coordinated complexes instead of pentacoordinated species analogous to **8i**. The cone angle of PPh<sub>3</sub> is large (145°),<sup>20</sup> and this results in a wide P-Pd-P angle for a cis-Pd(PPh<sub>3</sub>)<sub>2</sub> fragment (average 98°).<sup>21</sup> Because of the larger size of As the As-Pd-As is expected to be even larger (100.37°).<sup>22</sup> The bite angle of dppf in related allylic complexes (101.2°) is also large and shows a big difference with that of dppe (85.77°),<sup>23</sup> whose complex **2c** is a tetracoordinated σ-benzylic. In order to find out why the tetracoordinated σ-benzylic situation was not favored for **8**, we calculated several structures and computed their energy for **8i**. Neither complex **8i** nor any of its analogues could be crystallized and we were not able to determine their molecular structure. However, the collected experimental data tell us that **8i** is a pentacoordinated η<sup>3</sup>-benzylic species (see above) with a cis-PPh<sub>3</sub> (<sup>2</sup>J<sub>P,P</sub> = 51.9 Hz) and a trans-C<sup>α</sup>-P (<sup>2</sup>J<sub>C<sup>α</sup>,P</sub> = 50 Hz) arrangement. There are three isomeric forms that meet those requirements and they were minimized using the same methods described above (see also computational details in the Experimental and Supporting Information). As shown in Figure 4, the geometries found correspond to distorted square-pyramidal complexes with apical Br (**8i-spy-apiBr**) or apical PPh<sub>3</sub> (**8i-spy-apiPPh<sub>3</sub>**) and a complex that could be described as a very distorted trigonal bipyramid with axial PPh<sub>3</sub> and C<sup>α</sup> (**8i-dist-tbp**). All three structures are energetically favored when compared to the tetracoordinate σ-benzylic (**8i-4-coord-σ**), which also shows a significant deviation from the square planar geometry. The square pyramidal derivatives **8i-spy-apiBr** and **8i-spy-apiPPh<sub>3</sub>** are the most stable species, although the small energy difference found does not allow to favor one over the other (Figure 4). As observed before for **5i**, all the pentacoordinated η<sup>3</sup>-benzylic structures show analogous and significant differences in the distances Pd-C<sup>α</sup> (between 2.134-2.123 Å) and Pd-C2 (between 2.604-2.575 Å).<sup>12b</sup> The P-Pd-P angle is larger for the more stable **8i-spy-apiBr** (101°) and **8i-spy-apiPPh<sub>3</sub>** (102°) but smaller for **8i-dist-tbp** (97.3°). This angle is 99° for the tetracoordinated σ-benzylic. However moderate in value, the larger P-Pd-P angle in the square pyramidal pentacoordinated structures can alleviate the steric constraints imposed by the bulkiest ligands in a

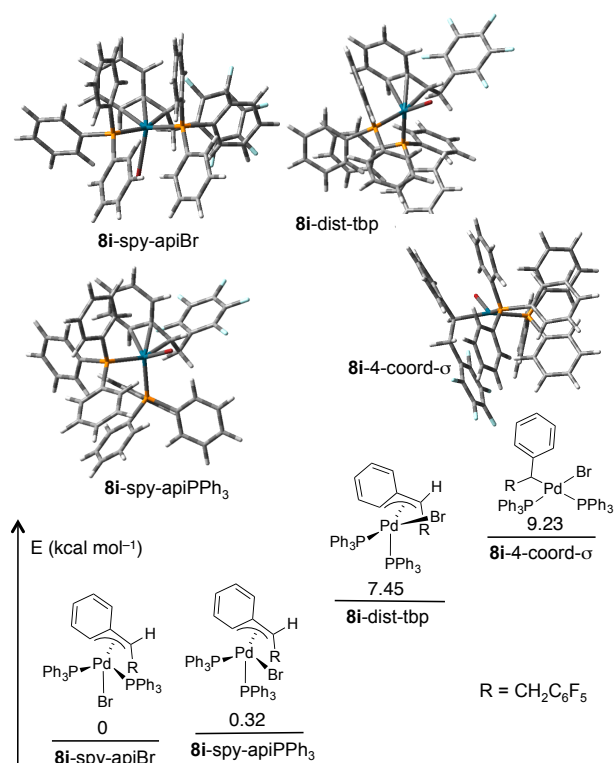


Figure 4. Calculated optimized structures of isomeric forms for **8i**. Selected geometrical parameters: P-Pd-P = 101° (**8i-spy-apiBr**), 102° (**8i-spy-apiPPh<sub>3</sub>**), 97.3° (**8i-dist-tbp**), 99° (**8i-4-coord-σ**).

cis arrangement, and, in contrast to what could be expected, favor an increase of the coordination number as a way to reach and overall less constrained geometry. Pentacoordination has also been observed in the solid state for η<sup>3</sup>-allyl or alkyl-olefin derivatives bearing the in-plane sterically demanding phenanthroline ligand.<sup>15b,c,16e</sup>

**Dynamic Behavior.** The benzylic complexes synthesized show a rich dynamic behavior in solution. The η<sup>3</sup>-σ-η<sup>3</sup> equilibrium that exchanges H<sup>2</sup> and H<sup>6</sup> in the phenyl ring observed of η<sup>3</sup>-benzylic complexes has been mentioned before. Other fluxional processes that involve ligand rearrangement operate when raising the temperature. The neutral complexes with two monodentate ligands undergo ligand exchange as the temperature is increased and the process is more clearly observed by <sup>31</sup>P{<sup>1</sup>H} NMR for the phosphino derivatives. For example, broadening of the phosphorous resonances of the PMe<sub>3</sub> occurs for complex **2a**, and also for both the trans and cis isomers of complex **2b** (Figure S6). As shown in Scheme 5, the benzylic group can play the role of an entering ligand through a change in coordination mode from σ (complexes **2** cis or trans) to η<sup>3</sup> leading to a pentacoordinated intermediate. A facial rotation on the trigonal bipyramid (turnstile movement) or two consecutive Berry pseudorotations can exchange the cis and trans isomers. Also a dissociation of a ligand can occur (Scheme 5).

The coalescence of the phosphorous resonances is also observed for the triphenylphosphine derivative **8i** as the temperature is raised. The AX spin system at 213 K becomes a broad signal at 273 K (Figure 5).<sup>24</sup> Upon addition of PPh<sub>3</sub> to **8i** at 233 K the broadening of the <sup>31</sup>P signal of free phosphine is also observed.

### Scheme 5. Ligand rearrangement processes in palladium benzylic complexes.

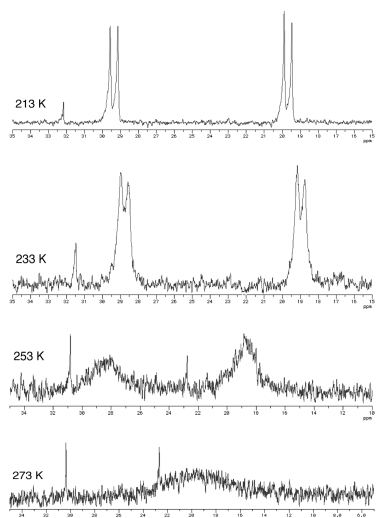
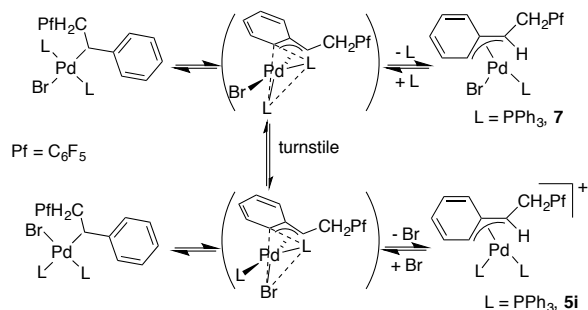


Figure 5. <sup>31</sup>P{<sup>1</sup>H} NMR spectrum of **8i** at different temperatures showing ligand exchange.

Thus, a ligand dissociation to a tetracoordinated  $\eta^3$  complex and subsequent recoordination contribute to the exchange (Scheme 5) and this should be very facile taking into account that the pentacoordinated intermediates, involved in these processes, are favored (complexes **8**). The calculated pentacoordinated complex **8i**-spy-apiBr is in fact the result of the reaction of **5i** with bromide as the entering ligand, and **8i**-spy-apiPPh<sub>3</sub> forms when **7** reacts with PPh<sub>3</sub> as the entering ligand. The other pentacoordinated structure **8i**-dist tbp or even the **8i**-4-ccord- $\sigma$  (Figure 4) are accessible in energy to participate in all the processes collected in Scheme 5 as the temperature raises.

Site exchange of both donor atoms has also been observed for complexes **2e<sub>1</sub>** and **2g** bearing chelating ligands. The ortho protons of the bipyridine ligand in **2e<sub>1</sub>** are inequivalent in the <sup>1</sup>H NMR spectrum at low temperature but coalesce at room temperature into a broad lump (Figure 6). However both halves of the bipy remain inequivalent for the minor isomer **2e<sub>2</sub>**. This difference also points to an associative exchange of nitrogens in the complex through a pentacoordinated intermediate formed by  $\eta^3$  coordination of the benzylic ligand (Figure 6). A turnstile twist in this intermediate and return to the  $\sigma$  mode could produce the observed effect. The adoption of  $\eta^3$  coordination is clearly more

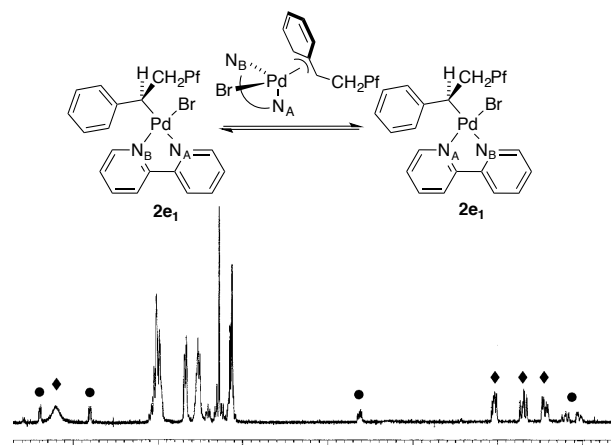


Figure 6. <sup>1</sup>H NMR spectrum of a mixture of **2e<sub>1</sub>** (◆) and **2e<sub>2</sub>** (●) at room temperature. The coalescence of H<sup>6</sup> and H<sup>6'</sup> of the bipy ligand in **2e<sub>1</sub>** is observed.

difficult when the  $\alpha$  aryl ring is a pentafluorophenyl as it is the case for the minor isomer. Thus, the pentafluorobenzyl group does not act as entering ligand and the exchange does not occur for **2e<sub>2</sub>**.

### CONCLUSIONS

A rich variety of coordination arrangements can be found for benzylic palladium complexes with an  $\alpha$ -substituent on the benzylic. The change in coordination mode from  $\eta^3$ - to  $\sigma$ -benzylic opens up a coordination site on palladium(II) that is generally and easily occupied by other ligands. Thus, complexes with composition [Pd(benzylic)BrL<sub>2</sub>] favor  $\sigma$ -benzylic coordination, except for the bromide (L = Br<sup>-</sup>), that would involve the formation of a dianionic species, and for the bulkiest ligands tried L = tri-arylphosphines or arsines. In this case a pentacoordinated  $\eta^3$ -benzylic coordination is preferred and calculations show that a square pyramidal structure is doable. The  $\eta^3$ -benzylic mode is retained to complete the coordination number of the metal in [Pd(benzylic)L<sub>2</sub>]<sup>+</sup> derivatives. When complexes with a [Pd(benzylic)BrL] composition are formed both  $\sigma$ -benzylic (**4**, L = tetrahydrothiophene) or  $\eta^3$ -benzylic (**7**, L = PPh<sub>3</sub>) coordination modes can be found.

The structural characterization of the number of representative complexes prepared seems to indicate that sterics play a fundamental role in the adoption of a coordination mode and a coordination number. The relief in steric constraints seems to be greater by adoption of an  $\eta^3$ -benzylic mode, even at the expense of increasing the coordination number of the metal to the less common 5-coordination (complexes **8**). The adoption of an anti isomeric form for the  $\alpha$ -substituted  $\eta^3$ -benzylics also leads to a less congested and more favorable situation, and indeed the anti isomer is found for the bulkiest auxiliary ligands (complexes **5i-k**). The interplay of the variety of coordination modes, some of them close enough in energy, favor the rich fluxional behavior found for these complexes that involve cis-trans isomerization, ligand exchange and  $\eta^3$ - to  $\sigma$ -benzylic rearrangement.

## EXPERIMENTAL SECTION

**General Methods.**  $^1\text{H}$ ,  $^{19}\text{F}$ ,  $^{13}\text{C}$  and  $^{31}\text{P}$  NMR spectra were recorded on Bruker AC-300, ARX-300 and AV-400 as well as Agilent MR-500 instruments. Chemical shifts (in  $\delta$  units, ppm) were referenced to  $\text{Me}_4\text{Si}$  ( $^1\text{H}$  and  $^{13}\text{C}$ ),  $\text{CFCl}_3$  ( $^{19}\text{F}$ ) and  $\text{H}_3\text{PO}_4$  (85%,  $^{31}\text{P}$ ). Signal assignments were made with the aid of heteronuclear  $^1\text{H}$ - $^{13}\text{C}$  HMQC and homonuclear  $^1\text{H}$  COSY and ROESY experiments. NMR data for the complexes can be found in Tables 1-4 and Table S1 in the Supporting Information. C, H and N elemental analyses were performed on a Perkin-Elmer 2400 CHN microanalyzer. Solvents were dried using a solvent purification system SPS PS-MD-5 or distilled from appropriate drying agents under nitrogen, prior to use. Complex **1** was prepared as previously reported.<sup>7</sup> Crystals of **2e**<sub>1</sub> and **2g** suitable for X-ray analyses were obtained by slow diffusion of n-hexane to a solution of each complex in  $\text{CH}_2\text{Cl}_2$  at  $-20^\circ\text{C}$ . The crystals were mounted on the tip of a glass fiber. X-ray measurements were made using Bruker SMART CCD area-detector diffractometer with Mo  $K\alpha$  radiation (0.71073 Å). Reflections were collected, intensities integrated, and the structures were solved by direct methods procedure. Non-hydrogen atoms were refined anisotropically and hydrogen atoms were constrained to ideal geometries and refined with fixed isotropic displacement parameters. Both complexes crystallized with a  $\text{CH}_2\text{Cl}_2$  molecule from the solvent mixture. Relevant crystallographic data are collected as Supporting Information.

### Synthesis of the neutral benzylic complexes.

**Synthesis of [PdBr( $\sigma$ -PhCHCH<sub>2</sub>C<sub>6</sub>F<sub>5</sub>)(PMe<sub>3</sub>)<sub>2</sub>] (2a).** To a suspension of complex **1** (0.05 g, 0.055 mmol) in  $\text{CH}_2\text{Cl}_2$  (3 mL) at 233 K was added a solution of  $\text{PMe}_3$  in THF (1M, 0.219 mL). The mixture was stirred and n-hexane (3 mL) was added to the resulting solution. The solvent was partially evaporated at 233 K until a solid precipitates, which was filtered and vacuum dried (0.055 g, 83% yield). Analysis calc. for  $\text{C}_{20}\text{H}_{26}\text{BrF}_5\text{P}_2\text{Pd}$ : C, 39.40; H, 4.30; found: C, 39.13; H, 4.03.

Complexes **2c**, **2e**, **2g** and **8k** were isolated in the same way. **2c**: Analysis calc. for  $\text{C}_{40}\text{H}_{32}\text{BrF}_5\text{P}_2\text{Pd}$ : C, 56.13; H, 3.77; N, 4.56; found: C, 55.96; H, 3.71; N, 4.58. **2e**: Analysis calc. for  $\text{C}_{24}\text{H}_{16}\text{BrF}_5\text{N}_2\text{Pd}$ : C, 46.97; H, 2.62; N, 4.56; found: C, 46.90; H, 2.52; N, 4.58. Slow crystallization of the complex from  $\text{CH}_2\text{Cl}_2$ /n-hexane gave crystals that contained a dichloromethane molecule; analysis calc. for  $\text{C}_{25}\text{H}_{18}\text{BrCl}_2\text{F}_5\text{N}_2\text{Pd}$ : C, 42.98; H, 2.59; N, 4.01; found: C, 42.97; H, 2.48; N, 4.03. **2g**: Analysis calc. for  $\text{C}_{28}\text{H}_{22}\text{BrF}_5\text{PdS}_2$ : C, 47.77; H, 3.15; found: C, 46.85; H, 2.91 ( $\text{CH}_2\text{Cl}_2$  is trapped in the crystal lattice). **8k**: Analysis calc. for  $\text{C}_{48}\text{H}_{36}\text{BrF}_5\text{FeP}_2\text{Pd}$ : C, 56.97; H, 3.59; found: C, 56.55; H, 3.41.

**Characterization of [PdBr( $\sigma$ -PhCHCH<sub>2</sub>C<sub>6</sub>F<sub>5</sub>)(P(OMe)<sub>3</sub>)<sub>2</sub>] (2b):** A suspension of **1** (0.018 g, 0.02 mmol) in  $\text{CDCl}_3$  (0.6 mL) was prepared in a 5 mm NMR tube and the tube was introduced in a cold bath at 223 K.  $\text{P(OMe)}_3$  (9.6  $\mu\text{L}$ , 0.079 mmol) was added to the suspension and the mixture was shaken and analyzed by multinuclear NMR. Complexes **2c**, **2d**, **2f**, **4** and **6-8** can be obtained in the same way using the corresponding Pd:ligand ratio. **2h** was prepared by addition of an excess of NCMe.

### Synthesis of the cationic benzylic complexes.

**Synthesis of [Pd( $\eta^3$ -PhCHCH<sub>2</sub>Pf)(AsPh<sub>3</sub>)<sub>2</sub>]BF<sub>4</sub> (5j).** Com-

plex **1** (0.3 g, 0.33 mmol) was added to a solution of  $\text{AgBF}_4$  (0.13 g, 0.65 mmol) and  $\text{AsPh}_3$  (0.40 g, 1.31 mmol) in acetone (20 mL) at 233 K. The suspension was stirred for 30 min protected from light and then it was filtered through magnesium sulfate at 233 K. The filtrate was evaporated to dryness and the residue was triturated with n-hexane (15 mL). The yellow product was filtered, washed with cold  $\text{Et}_2\text{O}$  (2 x 5 mL) and air-dried (0.5 g, 75 % yield). The complex was stored at  $-20^\circ\text{C}$ . Analysis calc. for  $\text{C}_{50}\text{H}_{38}\text{As}_2\text{BF}_9\text{Pd}$ : C, 55.77; H, 3.56; found: C, 55.99; H, 3.44.

Complexes **5c**, **5g**, **5i** and **5k** were prepared in a similar way using the appropriate ligand. **5c**: 74 % yield. Analysis calc. for  $\text{C}_{40}\text{H}_{32}\text{BF}_9\text{P}_2\text{Pd}$ : C, 55.68; H, 3.74; found: C, 55.36; H, 3.80. **5g**: 67 % yield. Analysis calc. for  $\text{C}_{28}\text{H}_{22}\text{BF}_9\text{PdS}_2$ : C, 47.32; H, 3.12; found: C, 47.15; H, 3.18. **5i**: 67 % yield. **5i**: Analysis calc. for  $\text{C}_{50}\text{H}_{38}\text{BF}_9\text{P}_2\text{Pd}$ : C, 60.72; H, 3.87; found: C, 60.19; H, 3.85. **5k**: 78 % yield. Analysis calc. for  $\text{C}_{48}\text{H}_{36}\text{BF}_9\text{FeP}_2\text{Pd}$ : C, 56.59; H, 3.56; found: C, 56.53; H, 3.52.

**Characterization of [PdBr( $\sigma$ -PhCHCH<sub>2</sub>Pf)(CD<sub>3</sub>CN)<sub>3</sub>]BF<sub>4</sub> (3h):**  $\text{AgBF}_4$  (0.0256 g, 0.0132 mmol) was added to a solution of **1** (0.0602 g, 0.066 mmol) in  $\text{CD}_3\text{CN}$  (1.5 mL) at room temperature. The mixture was stirred for 5 min and the resulting suspension was filtered. The filtrate, containing complex **3h**, was analyzed by NMR.

**Characterization of [PdBr( $\eta^3$ -PhCHCH<sub>2</sub>Pf)(PMe<sub>3</sub>)<sub>2</sub>]BF<sub>4</sub> (5a).** Method A:  $\text{AgBF}_4$  (0.0097 g, 0.05 mmol) was added to a solution of complex **2a** (0.016 mmol) in  $\text{CDCl}_3$  (0.6 mL) at 233 K. The suspension was shaken and it was analyzed by NMR. Method B:  $\text{AgBF}_4$  (0.005 g, 0.026 mmol) was added to a solution of complex **2a** (0.017 mmol) in acetone (2 mL) at 233 K. After stirring for 10 min, the  $\text{AgBr}$  formed was filtered and the filtrate was evaporated to dryness. The residue was dissolved in  $\text{CDCl}_3$  (0.6 mL) and the complex in solution was characterized by NMR.

Complex **5f** was prepared by method A and **5a**, **5d** can be prepared using either method.

**Computational details.** All calculations were performed using the DFT approach with the M06 functional<sup>25,26</sup> using Gaussian09 as program package.<sup>27</sup> The selected basis set was 6-31+G(d) for C, P, F, H,<sup>28,29</sup> LANL2DZ ECP for the Br and SDD for Pd<sup>30,31</sup> (Basis set I). Solvation was introduced through the SMD model, where we applied dichloromethane as the solvent ( $\epsilon = 9.1$ ). All geometry optimizations were carried out in solution with no restrictions. Free energy corrections were calculated at 298.15 K and  $10^5$  Pa pressure, including zero point energy corrections (ZPE). Vibrational frequency calculations were performed to establish the stationary points were minima (without imaginary frequencies) or transition states (with one imaginary frequency). Final potential energies were refined by performing additional single-point energy calculations, Pd was described with SDD def2-QZVP, the Br atom was described with LANL2DZ ECP and the remaining atoms were treated with 6-311++G\*\* basis set (Basis set II). All reported energies in the manuscript correspond to Gibbs energies in solution, obtained from potential energies (including solvation) with basis set II plus Gibbs energy corrections with basis set I.

**Table 1: <sup>1</sup>H NMR data for the  $\sigma$ -benzyl palladium derivatives.<sup>a</sup>**

Complex	T	H <sup><math>\alpha</math></sup> (J)	H <sup><math>\beta</math></sup> (J)	H <sup><math>\beta'</math></sup> (J)	H <sup>2</sup> / H <sup>6</sup>	Other
<b>2a</b>	233 K	4.26 m	3.19 m	3.19 m	7.37 d (6.9)	1.25 (m, 18H, Me), 7.08 (t, J = 6.9, 1H, H <sup>4</sup> ), 7.23 (t, J = 6.9, 2H, H <sup>3,5</sup> )
<b>trans-2b<sup>b</sup></b>	223 K	4.79 m	3.80 m	2.92 m	7.30 m	3.62 (b, 18H, OMe), 7.13 (m, 1H, H <sup>4</sup> ), 7.23 (m, 2H, H <sup>3,5</sup> )
<b>2c</b>	293 K	3.36 m	4.17 m (14.2, 11.5)	3.57 m (14.2, 4.8)	7.2-7.9	1.75-2.55 (m, 4H, CH <sub>2</sub> dppe), 6.86 (b, 5H, H <sup>4</sup> , Ph dppe), 7.2-7.9 (m, 18H, H <sup>3</sup> , H <sup>5</sup> , Ph dppe)
<b>trans-2d</b>	223 K	3.83 t (7.3)	3.22 dd (14.0, 7.3)	2.55 dd (14.0, 7.3)	6.79 d (6.7)	7.01 (t, 2H, H <sup>3,5</sup> ), 7.07 (t, 1H, H <sup>4</sup> ), 7.30 (t, J = 6.7, 4H, H <sub>meta</sub> py), 7.79 (t, J = 6.7, 2H, H <sub>para</sub> py), 8.52 (t, 4H, H <sub>ortho</sub> py)
<b>cis-2d</b>	273 K	3.83 m	3.55 m	3.10 m	6.8-7.4	6.8-7.4 (m, 3H, H <sup>3,4,5</sup> ), 7.20 (m, 2H, H <sub>meta</sub> py), 7.38 (m, 2H, H <sub>meta</sub> py), 7.65 (m, 2H, H <sub>para</sub> py), 8.12 (bs, 2H, H <sub>ortho</sub> py), 8.52 (bs, 2H, H <sub>ortho</sub> py)
<b>2e<sub>1</sub></b>	293 K	3.93 dd (9.5, 5.9)	3.68 dd (14.1, 9.5)	3.39 dd (14.1, 5.9)	7.65 d (6.5)	7.12 (m, 3H, H <sup>3,4,5</sup> ), 7.98 (m, 4H, H <sup>3,4,3',4'</sup> bipy), 7.50 (m, 2H, H <sup>5,5'</sup> bipy), 9.10 (a, 2H, H <sup>6,6'</sup> bipy)
<b>2e<sub>2</sub></b>	293 K	5.57 dd (10.4, 5.2)	3.13 dd (13.8, 10.3)	3.02 dd (13.8, 5.2)	7.1-8.1	7.1-8.1 (m, 3H, H <sup>3,4,5</sup> ), 7.39 (t, 1H, H <sup>5</sup> bipy), 7.50 (t, 1H, H <sup>5'</sup> bipy), 7.98 (m, 4H, H <sup>3,4,3',4'</sup> bipy), 8.75 (d, 1H, H <sup>6</sup> bipy), 9.33 (d, 1H, H <sup>6'</sup> bipy)
<b>2f</b>	223 K	4.35 b	3.35 bt	2.85 b	7.1-7.5 m	2.01 (bs, 8H, H <sup>3,4</sup> tht), 2.85 (a, 8H, H <sup>2,5</sup> tht), 7.1-7.5 (m, 3H, H <sup>3,4,5</sup> )
<b>2g</b>	293 K	5.47 dd (9.6, 5.2)	3.72 t (14.3)	2.88 m	7.34 m	2.6-3.1 (m, 4H, CH <sub>2</sub> S), 6.69 (t, J = 7.4, 1H, H <sup>4</sup> ), 6.81 (t, J = 7.4, 2H, H <sup>3,5</sup> ), 7.27 (m, 4H, H <sub>meta</sub> Ph), 7.32 (m, 2H, H <sub>para</sub> Ph), 7.58 (m, 4H, H <sub>ortho</sub> Ph)
<b>2h</b>	293 K	4.32 t (7.6)	3.25 dd (13.9, 7.6)	2.70 dd (13.9, 7.6)	7.25 b	7.4 (m, 3H, H <sup>3,4,5</sup> )
<b>3h</b>	243 K	4.33 t (7.8)	3.22 dd (14.8, 8.2)	2.59 dd (14.8, 7.4)	7.50 d (7.5)	7.29 (m, 2H, H <sup>3,5</sup> ), 7.34 (m, 1H, H <sup>4</sup> )
<b>3d<sup>c</sup></b>	233 K	3.60t (7.6)	3.38dd (14.4, 7.5)	2.66 dd (14.4, 8.8)	6.87 m	6.97 (m, 2H, H <sup>3,5</sup> ), 7.01 (t, 1H, H <sup>4</sup> ), 7.22 (m, 2H, H <sub>meta</sub> py trans), 7.38 (m, 4H, H <sub>meta</sub> py cis), 7.66 (t, 1H, H <sub>para</sub> py trans), 7.84 (t, 2H, H <sub>para</sub> py cis), 8.33 (m, 2H, H <sub>ortho</sub> py trans), 8.57 (d, 4H, H <sub>ortho</sub> py cis)
<b>4</b>	223 K	4.87	3.30	2.89	7.21 a	1.5-3.3 (m, 8H, tht), 7.38 (a, 3H, H <sup>3,4,5</sup> )

a)  $\delta$ , 300 MHz; spectra recorded in CDCl<sub>3</sub> except for **2h**, **3h** and **3d** (CD<sub>3</sub>CN). b) The characterization of **cis-2b** was not possible due to the low intensity of the signals. c) 500 MHz

**Table 2: <sup>13</sup>C NMR data for the palladium benzyl derivatives.<sup>a</sup>**

Complex	T	C <sup><math>\alpha</math></sup>	<sup>1</sup> J <sub>C<sup><math>\alpha</math></sup>-H</sub>	C <sup><math>\beta</math></sup>	<sup>1</sup> J <sub>C<sup><math>\beta</math></sup>-H</sub>	<sup>2</sup> J <sub>C<sup><math>\alpha</math></sup>-P</sub>	C <sup>1</sup>	C <sup>2</sup> /C <sup>6</sup>	C <sup>3</sup> /C <sup>5</sup>	C <sup>4</sup>
<b>2a</b>	263 K	30.95	134.1	27.54	132.4	< 18	149.23	126.57	127.87	124.39
<b>trans-2b</b>	233 K	37.28	142.6	26.60	131.3	< 18	148.21	126.87	127.78	124.55
<b>2c</b>	223 K	42.91	140.1	29.95	135.5	101.9	145.82	126.90	127.64	123.42
<b>trans-2d</b>	263 K	37.44	140.4	26.05	130.6	----	146.99	124.98	125.08	123.95
<b>2e<sub>1</sub></b>	293 K	37.43	*	30.55	*	----	138.8	126.19	127.99	124.58
<b>2g</b>	293 K	41.31	150	28.42	132	----	146.6	126.6	128.32	124.88
<b>2h<sup>b</sup></b>	263 K	43.45	*	24.06	131.9	----	*	115.16	127.02	130.34
<b>3h<sup>c,d</sup></b>	233 K	36.80	145.2	26.72	139	----	143.6	127.5	129.38	126.6
<b>3d</b>	233 K	38.22	137	30.7	131.4	----	152.5	130.9	133.7	129.3
<b>4</b>	223 K	37.10	*	26.18	136.0	----	145.35	126.08	128.46	125.41
<b>5a</b>	223 K	62.05	160.2	22.21	137.3	43.6	118.08	103.04/127.60	129.81/132.09	133.66
<b>5c</b>	223 K	63.82	156.4	21.52	133.0	45.8	120.65	113.17/110.20	*	*
<b>5f</b>	213 K	65.2	*	22.59	137.3	----	116.3	*	133.8	133.07
<b>5g<sup>d</sup></b>	293 K	67.80	155	23.14	136	----	----	132.7	----	----
<b>5i</b>	223 K	70.48	156.0	21.19	132.5	53.0	118.46	107.03/126.3	133.02/*	132.3
<b>5j</b>	243 K	68.34	158.5	21.59	135.8	----	115.66	108.21/123.8	*	*
<b>5k</b>	223 K	68.94	----	20.60	----	70.0	*	105/	134.5	*
<b>6</b>	233 K	54.59	154.7	*	*	----	98.5	*	*	*
<b>7</b>	233 K	59.65	155.4	21.78	133.4	< 20	*	134/	*	*
<b>8i</b>	223 K	60.63	155.0	24.84	133.2	50.0	*	*	*	*
<b>8j</b>	243 K	54.68	*	23.27	136.0	----	*	118.56	*	*
<b>8k</b>	223 K	58.91	150.0	25.80	134	71.0	----	----	----	----

a)  $\delta$ , 75 MHz; spectra recorded in CDCl<sub>3</sub> unless otherwise noted. The signals and coupling constants that could not be assigned due to signal overlap or low intensity resonances are marked with an asterisk. b) Spectra recorded in mixture CDCl<sub>3</sub>/CD<sub>3</sub>CN. c) Signals corresponding to the C<sub>6</sub>F<sub>5</sub> group are also visible in this spectrum: 145 (m, <sup>1</sup>J<sub>C-F</sub> = 245 Hz, C<sub>ortho</sub>), 139.67 (m, <sup>1</sup>J<sub>C-F</sub> = 252 Hz, C<sub>para</sub>), 137.42 (m, <sup>1</sup>J<sub>C-F</sub> = 247 Hz, <sup>2</sup>J<sub>C-F</sub> = 16 Hz, C<sub>meta</sub>), 113.25 (t, <sup>2</sup>J<sub>C-F</sub> = 20 Hz, C<sub>ipso</sub>). d) 125 MHz.

**Table 3: <sup>1</sup>H NMR data for the η<sup>3</sup>-benzyl derivatives.<sup>a</sup>**

Complex	T	H <sup>α</sup> (J)	H <sup>β</sup> (J)	H <sup>β'</sup> (J)	H <sup>2</sup> / H <sup>6</sup>	Other
<b>5a</b>	223 K	3.60 m	3.09 m	3.09 m	6.82 m	1.20 (d, 9H, J = 9.8, Me), 1.72 (d, 9H, J = 8.8, Me), 7.46 (m, 2H, H <sup>3,5</sup> ), 7.83 (m, 1H, H <sup>4</sup> )
<b>5c</b>	223 K	4.02 t (10.5)	2.95 m	2.66 m	6.53 b / 7.15 m	7.50 (m, 2H, H <sup>3,5</sup> ), 7-7.9 (m, 21H, H <sup>4</sup> , Ph dppe)
<b>5d</b>	293 K	3.78 dd (9.4, 5.4)	3.08 dd (14.8, 9.4)	2.69 bd (14.8)	6.70 b / 7.40 m	7.2-7.8 (m, 3H, H <sup>3,4,5</sup> ), 7.32 (m, 2H, H <sub>meta</sub> py), 7.44 (m, 2H, H <sub>meta</sub> py), 7.70 (ta, 1H, H <sub>para</sub> py), 7.85 (bs, 1H, H <sub>para</sub> py), 8.14 (bs, 2H, H <sub>ortho</sub> py), 8.65 (bs, 2H, H <sub>ortho</sub> py)
<b>5f</b>	223 K	3.75 m	3.38 m	3.14 m	6.76 m / 7.47 m	1.91 (b, 4H, tht), 2.15 (b, 2H, tht), 2.59 (b, 2H, tht), 2.82 (b, 2H, tht), 3.35 (b, 4H, tht), 3.57 (b, 2H, tht), 7.56, 7.64 (bt, bt, 2H, H <sup>3,5</sup> ), 7.78 (m, 1H, H <sup>4</sup> )
<b>5g</b>	293 K	4.35 m	3.32 m	3.20 m	7.15 m	3.10 (m, 4H, CH <sub>2</sub> S), 7.35, 7.4, 7.52 (m, 9H, H <sup>3,4,5</sup> , H <sub>meta,para</sub> Ph, H <sub>ortho</sub> Ph), 7.60 (m, 2H, H <sub>meta</sub> Ph), 7.77, (m, 2H, H <sub>ortho</sub> Ph)
<b>5i</b>	223 K	3.92 m	3.23 bt (12.9)	2.46 bd (12.9)	6.77 m / 7.11 d	6.38 t (J = 7.1, 1H, H <sup>3</sup> ) 6.71 (m, 6H, Ph PPh <sub>3</sub> ), 6.98 (bt, 1H, H <sup>4</sup> ), 7.15-7.5 (m, 24H, Ph PPh <sub>3</sub> , H <sup>5</sup> )
<b>5j</b>	223 K	4.27 dd (12, 4.2)	3.30 t (13.4)	2.58 bd (13.4)	6.89 d (8) / 7.09 d (8)	6.78 (t, J = 8.0, 1H, H <sup>3</sup> ) 6.87 (m, 6H, Ph AsPh <sub>3</sub> ), 7.18-7.43 (m, 26H, Ph PPh <sub>3</sub> , H <sup>5</sup> , H <sup>4</sup> )
<b>5k</b>	223 K	3.81 m	3.02 m	2.19 m	6.76 / 7	3.64, 3.96, 4.25, 4.35, 4.47, 4.78, 4.95 (s, 8H, Cp), 6.52 (m, 1H, H <sup>3</sup> ), 6.67 (m, 2H, Ph dppf), 7 (m, 3H, H <sup>6</sup> , Ph dppf), 7.15-7.75 (m, 18H, H <sup>5</sup> , H <sup>4</sup> , Ph dppf)
<b>6</b>	293 K	3.58 m	3.45 m	3.02 m	6.70 b	7.40 (b, 3H, H <sup>3,4,5</sup> )
<b>6</b>	223 K	3.48 m	3.48 m	3.05 m	6.03 b / 7.15 b	7.38 (b, 3H, H <sup>3,4,5</sup> )
<b>7</b>	213 K	3.62 bd (9.5)	2.90 bt (12.0, 9.5)	2.01 bd (12.0)	6.97 b / 7.2-7.9 m	7.2-7.9 (m, 19H, H <sup>3,4,5,6</sup> , PPh <sub>3</sub> )
<b>8i</b>	213 K	3.54 bd (9.0)	3.86 ta (13, 9)	2.94 bd (13.0)	6.77 m	6.9-7.7 (m, 33H, H <sup>3,4,5</sup> , PPh <sub>3</sub> )
<b>8k</b>	223 K	3.41 m	3.70 m	3.07 m	7.0-8.0 m	3.37, 3.44, 4.15, 4.32, 4.48, 4.51, 4.57 (s, 8H, Cp), 7.0-8.0 (m, 23H, H <sup>3</sup> , H <sup>5</sup> , H <sup>4</sup> , Ph dppf)
<b>8j</b>	263 K	3.82 m	2.93 t (12.3)	2.5 b	7.12 m	7.3-7.8 (a, 33H, H <sup>3,4,5</sup> , AsPh <sub>3</sub> )

a) δ, 300 MHz; spectra recorded in CDCl<sub>3</sub>.

**Table 4: <sup>31</sup>P NMR data for the palladium benzyl derivatives.<sup>a</sup>**

Complex	T	P <sub>A</sub>	P <sub>B</sub>	J <sub>P-P</sub> (Hz)
<b>2a</b>	223 K	-15.54 bs	-15.54 bs	
<i>cis</i> - <b>2b</b> <sup>b</sup>	233 K	131.35 d	120.06 d	137
<i>trans</i> - <b>2b</b>	233 K	119.80	119.00	250
<b>2c</b>	293 K	54.66 d	37.83 d	41.9
<b>5a</b>	223 K	-7.45 d	-24.97 d	49.9
<b>5c</b>	223 K	54.15 d	46.80 d	43.0
<b>5i</b>	213 K	32.75 d	23.30 d	47.0
<b>5k</b>	223 K	32.12	20.75	51.5
<b>7</b>	213 K	33.63	-----	-----
<b>8i</b>	213 K	29.35 d	19.68 d	51.9
<b>8k</b>	223 K	31.35 d	16.49 d	55.1

a) δ, 121 MHz; spectra recorded in CDCl<sub>3</sub>. b) The analysis was made using a spin system simulation.

## ASSOCIATED CONTENT

### Supporting Information

The Supporting Information is available free of charge on the ACS Publications website. It contains a PDF file with <sup>19</sup>F NMR spectral data for all the complexes, crystallographic data, additional figures and computational information with cartesian coordinates of calculated structures (XYZ).

## AUTHOR INFORMATION

E-mail: albeniz@qi.uva.es

## ACKNOWLEDGMENT

Financial support from the Spanish MINECO (SGPI, grant CTQ2016-80913-P) is gratefully acknowledged. We are indebted to Prof. Agustí Lledós (Universidad Autónoma de Barcelona) for his help with the DFT calculations.

This work is dedicated to Prof. Peter M. Maitlis on occasion of his 85th birthday. We are indebted to him for his impressive contribution to organometallic chemistry that has inspired many of us.

## REFERENCES

- (1) Recent reviews: a) Trost, B. M.; Czabaniuk, L. C. Structure and Reactivity of Late Transition Metal η<sup>3</sup>-Benzyl Complexes. *Angew. Chem. Int. Ed.* **2014**, *53*, 2826–2851; b) Liégault, B.; Renaud, J.-L.; Bruneau, C. Activation and functionalization of benzyl derivatives by palladium catalysts. *Chem. Soc. Rev.* **2008**, *37*, 290–299. Recent examples: c) Yang, M. -H.; Hunt, J. R.; Sharifi, N.; Altman, R. A. Palladium Catalysis Enables Benzoylation of α,α-Difluoroketone Enolates. *Angew. Chem. Int. Ed.* **2016**, *55*, 9080–9083. d) Najib, A.; Hirano, K.; Miura, M. Palladium-Catalyzed Asymmetric Benzyl Substitution of Secondary Benzyl Carbonates with Nitrogen and Oxygen Nucleophiles. *Org. Lett.* **2017**, *19*, 2438–2441.
- (2) LaPointe, A. M.; Rix, F. C.; Brookhart, M. Mechanistic Studies of Palladium(II)-Catalyzed Hydrosilylation and Dehydrogenative Silation Reactions. *J. Am. Chem. Soc.* **1997**, *119*, 906-917.
- (3) a) Trzeciak, A. M.; Ciunik, Z.; Ziolkowski, J. J. Synthesis of Palladium Benzyl Complexes from the Reaction of PdCl<sub>2</sub>[P(OPh)<sub>3</sub>]<sub>2</sub> with

Benzyl Bromide and Triethylamine: Important Intermediates in Catalytic Carbonylation. *Organometallics* **2002**, *21*, 132-137. b) Narahashi, H.; Shimizu, I.; Yamamoto, A. Synthesis of benzylpalladium complexes through C–O bond cleavage of benzylic carboxylates: Development of a novel palladium-catalyzed benzylation of olefins. *J. Organomet. Chem.* **2008**, *693*, 283–296.

(4) Rix, F. C.; Rachita, M. J.; Wagner, M. I.; Brookhart, M.; Milani, B. Barborak, J. C. Palladium(II)-catalyzed copolymerization of styrenes with carbon monoxide: mechanism of chain propagation and chain transfer. *Dalton Trans.* **2009**, 8977–8992.

(5) Hikawa, H.; Koike, T.; Izumi, K.; Kikkawa, S.; Azumaya, I. Borrowing Hydrogen Methodology for N-Benzylation using a  $\pi$ -Benzylpalladium System in Water. *Adv. Synth. Catal.* **2016**, *358*, 784–791.

(6) Johns, A. M.; Utsunomiya, M.; Incarvito, C. D.; Hartwig, J. F. A. Highly Active Palladium Catalyst for Intermolecular Hydroamination. Factors that Control Reactivity and Additions of Functionalized Anilines to Dienes and Vinylarenes. *J. Am. Chem. Soc.* **2006**, *128*, 1828–1839.

(7) Albéniz, A. C.; Espinet, P.; Lin, Y. –S. Involvement of Intramolecular Hydride Transfer in the Formation of Alkanes from Palladium Alkyls. *Organometallics*, **1997**, *16*, 4030–4032.

(8) The trans:cis equilibrium is solvent dependent; a trans:cis = 2.3:1 ratio was observed for 2b in acetone, the more polar the solvent the higher the amount of the more polar cis derivative.

(9) Rix, F. C.; Brookhart, M.; White, P. S. Electronic Effects on the  $\beta$ -Alkyl Migratory Insertion Reaction of *para*-Substituted Styrene Methyl Palladium Complexes. *J. Am. Chem. Soc.* **1996**, *118*, 2436–2448.

(10) Deviations from planarity in bipy complexes have been long known and they seem to occur in order to avoid the steric repulsions between the H6 protons of bipyridine (spanning on the metal coordination plane) and the other ligands; see for example: a) McKenzie, E. D. The steric effect in bis(2,2'-bipyridyl) and bis(1,10-phenanthroline) metal compounds. *Coord. Chem. Rev.* **1971**, *6*, 187–216. b) Chieh, P. C. Crystal and molecular structure of aquobis-(2,2'-bipyridyl)palladium dinitrate. *J. Chem. Soc. Dalton Trans.* **1972**, 1643–1646.

(11) The exchange between the dimeric complexes probably occurs by cleavage and re-formation of the bromo bridges. This process may easily involve intermediate  $\eta^3$ -benzyls that aid the bridge cleavage.

(12) a) Becker, Y.; Stille, J. K. The Dynamic  $\eta^1$ - and  $\eta^3$ -Benzylbis(triethylphosphine)palladium(II) Cations. Mechanisms of Interconversion. *J. Am. Chem. Soc.* **1978**, *100*, 845–850. b) Craswell, L. E.; Spencer, J. L. Preparation and Fluxional Behaviour of  $\eta^3$ -Methylbenzyl Platinum and Palladium Complexes. *J. Chem. Soc., Dalton Trans.*, **1992**, 3445–3452. c) Gatti, G.; López, J. A.; Mealli, C.; Musco, A. Structural and NMR spectroscopic characterization of  $\eta^3$ -Benzyl palladium(II) complexes. *J. Organomet. Chem.* **1994**, *483*, 77–89.

(13) (a) Sonodo, A.; Bailey, P. M.; Maitlis, P. M. Crystal and Molecular Structures of Pentane-2,4-dionato-( $\alpha$ ,1,2- $\eta$ -tri-phenylmethyl)-palladium and -platinum. *J. Chem. Soc. Dalton Trans.* **1979**, 346–350.

b) Stühler, H.-O. (1,2,5,6- $\eta$ -1,5-Cyclooctadiene)-(1,2,7- $\eta$ -7-methylbenzyl)(7,8- $\eta$ -styrene)rhodium(I)—Antarafacial Fluctuation of the Benzyl Ligand and Temperature-Dependent Coordination of Styrene. *Angew. Chem. Int. Ed. Engl.* **1980**, *19*, 468–469. c) Su, S.-C. H.; Wojcicki, A. Stereochemical Studies on Thermal and Photochemical Reactions of  $\eta^3$ -C<sub>6</sub>H<sub>5</sub>W(CO)(phenethyl) Containing Deuterium-Labeled Phenethyl Ligands. *Organometallics* **1983**, *2*, 1296–1301. d) Carmona, E.; Paneque, M.; Poveda, M. L. Synthesis and Characterization of Some New Organometallic Complexes of Nickel(II) Containing Trimethylphosphine. *Polyhedron*, **1989**, *8*, 285–291. e) Cámpora, J.; Carmona, E.; Gutiérrez, E.; Poveda, M. L.; Ruiz, C. Binuclear  $\sigma$ - and  $\eta^3$ -Benzylic Derivatives of Nickel. *J. Chem. Soc. Dalton Trans.* **1992**, 1769–1774.

(14) Pentacoordinated palladium(II) complexes are not common but representative examples have been long known: Albéniz, A. C.; Espinet, P. Palladium: Inorganic & Coordination Chemistry, in *Encyclopedia of*

*Inorganic Chemistry*, editor-in-chief, King, R. B.; England; **1994**, *6*, 3018.

(15) Selected examples of trigonal bipyramidal Pd(II) compounds (other than those with specially designed tripod ligands): a) Konietzny, A.; Bailey, P. M.; Maitlis, P. M. The Cyclotetramerisation of Dimethyl Acetylenedicarboxylate and the X-Ray Structure of [Pd{H(C<sub>8</sub>(CO<sub>2</sub>Me)<sub>2</sub>)<sub>2</sub>}Cl(pyridine)<sub>2</sub>], an Unusual Five-coordinate Palladium(II) Complex. *J. Chem. Soc. Chem. Commun.* **1975**, 78–79. b) Albano, V. G.; Castellar, C.; Cucciolino, M. E.; Panunzi, A.; Vitagliano, A. Synthesis and Characterization of Five-Coordinate Olefin Complexes of Palladium(II). Molecular Structure of the Acetone Solvate of (2,9-Dimethyl-1,10-phenanthroline)(maleic anhydride)methylchloro palladium. *Organometallics*, **1990**, *9*, 1269–1276. c) Burger, P. Baumeister, J. M. Transition metal complexes with sterically demanding ligands. I. Synthesis and X-ray crystal structure of 1,5-cyclooctadiene palladium methyl triflate, (COD)Pd(Me)(OTf) and its cationic penta-coordinate adducts with sterically demanding 2,9-diaryl-substituted 1,10-phenanthroline ligands. *J. Organomet. Chem.* **1999**, *575*, 214–222. d) López-Torres, M.; Fernández, A.; Fernández, J. J.; Suárez, A.; Pereira, M. T.; Ortigueira, J. M.; Adams, H. Mono- and Dinuclear Five-coordinate Cyclometalated Palladium(II) Compounds. *Inorg. Chem.* **2001**, *40*, 4583–4587. e) Binotti, B.; Bellachio, G.; Cardaci, G.; Macchioni, A.; Zuccaccia, C.; Foresti, E.; Sabatino, P. Intramolecular and Interionic Structural Studies of Novel Olefin Palladium(II) and Platinum(II) Complexes Containing Poly(pyrazol-1-yl)borate and -methane Ligands. X-ray Structures of Palladium Five-Coordinate Complexes. *Organometallics* **2002**, *21*, 346–354. f) Bedford, R. B.; Betham, M.; Butts, C. P.; Coles, S. J.; Cutajar, M.; Gelbrich, T.; Hursthouse, M. B.; Scully, P. N.; Wimperis, S. Five-coordinate Pd(II) orthometalated triarylphosphite complexes. *Dalton Trans.*, **2007**, 459–466. g) Kirai, N.; Takaya, J.; Iwasawa, N. Two Reversible  $\sigma$ -Bond Metathesis Pathways for Boron–Palladium Bond Formation: Selective Synthesis of Isomeric Five-Coordinate Borylpalladium Complexes. *J. Am. Chem. Soc.* **2013**, *135*, 2493–2496.

(16) Square pyramidal Pd(II) derivatives: a) Collier, J. W.; Mann, F. G.; Watson, D. G.; Watson, H. R. The Constitution of Complex Metallic Salts. Part XIX. The 2-Phenylisophosphindoline Derivatives of Platinum(II), Palladium(II) and Nickel(II). *J. Chem. Soc.* **1964**, 1803–1814. b) Chui, K. M.; Powell, H. M. Pyramidal Five-coordinate with Flattened Tetrahedral Basal Bonds. Crystal and Molecular Structures of Dibromotris-(5-ethyl-5H-dibenzo-phosphole)palladium(II)-Chlorobenzene, Dibromotris-(5-ethyl-5H-di-benzophosphole)-platinum(II)-Bromobenzene, and Dibromotris-(5-methyl-5H-dibenzo-phosphole)-platinum(II)-Bromobenzene. *J. Chem. Soc. Dalton Trans.*, **1974**, 1879–1889. c) Chui, K. M.; Powell, H. M. Comparison of Stereochemistry in Racemic and Optically Resolved Forms of a Five-coordinate Compound. Crystal and Molecular Structures of Dibromotris-(2-phenylisophosphindoline)palladium(II)-Acetone (Orange) and Dibromotris-(2-phenylisophosphindoline)palladium(II) (Red). *J. Chem. Soc. Dalton Trans.*, **1974**, 2117–2122. d) Louw, W. J.; de Waal, D. J. A. Preparation of the Five-coordinate Complexes [PdX<sub>2</sub>(PMe,Ph)<sub>3</sub>] (X = Cl, Br, or I) and the Crystal and Molecular Structure of Dichlorotris-[dimethylphenylphosphine]palladium. *J. Chem. Soc. Dalton Trans.*, **1976**, 2364–2368. e) Hansson, S.; Norrby, P.-O.; Sjögren, M. P. T.; Åkermark, B.; Cucciolito, M. E.; Giordano, F.; Vitagliano, A. Effects of Phenanthroline Type Ligands on the Dynamic Processes of ( $\eta^3$ -Allyl)palladium Complexes, Molecular Structure of (2,9-Dimethyl-1,10-phenanthroline)[(1,2,3- $\eta$ )-3-methyl-2-butenyl]-chloropalladium. *Organometallics*, **1993**, *12*, 4940–4948. f) Bröring, M.; Brandt, C. D. A five coordinate Pd<sup>II</sup> complex stable in solution and in the solid state. *Chem. Commun.* **2003**, 2156–2157. g) Zhang, X.; Xia, Q.; Chen, W. Synthesis of tetra- and pentacoordinate palladium complexes of functionalized N-heterocyclic carbenes and a comparative study of their catalytic activities. *Dalton Trans.*, **2009**, 7045–7054.

(17) Rülke, R. E.; Ernsting, J. M.; Spek, A. L.; Elsevier, C. J.; van Leeuwen, P. W. N. M.; Vrieze, K. NMR Study on the Coordination

Behavior of Dissymmetric Terdentate Trinitrogen Ligands on Methylpalladium(II) Compounds. *Inorg. Chem.* **1993**, *32*, 5769-5778.

(18) Suitable crystals for a high quality X-ray crystal structural determination could not be obtained for **5k**. However, a disordered molecular structure (the disorder affecting mainly, but not only, to the anion and solvent molecules of crystallization) was obtained which could not be completely refined ( $R = 12\%$ ). It shows the structure of an anti- $\eta^3$ -benzylic complex. See supporting information.

(19) Geometries were calculated for two different relative locations of the cation and anion, labeled up and down relative to the  $C_{\text{ipso}}$  benzylic carbon. All the structures and the calculated energies are collected in the Supporting Information. There is no significant energy difference for the up or down  $\text{BF}_4^-$  structures for each isomer (less than 1 kcal/mol), the down location being always more stable. Thus, the energy differences between the syn and anti isomers are given in Figure 3 for the down  $\text{BF}_4^-$  location.

(20) Tolman, C. A. Steric Effects of Phosphorus Ligands in Organometallic Chemistry and Homogeneous Catalysis. *Chem. Rev.* **1977**, *77*, 313-348.

(21) Cambridge Structural Database System (CSD System, version 5.38, **2016**). Cambridge Crystallographic Data Centre, 12 Union Road, Cambridge CB2 1EZ, UK.

(22) Kemmitt, R. D. W.; McKenna, P.; Russell, D. R.; Sherry, L. J. S. Chemistry of Metallacyclobutanones. Part 2. Synthesis and Ring Inversion of some Highly Puckered Metallacyclobutan-3-one (Slipped Oxodimethylenemethane) Complexes of Palladium; Crystal Structures of 2,4-Bis(methoxycarbonyl)-1,1-bis(triphenylphosphine)-palladacyclobutan-3-one, 2,4-bis(methoxycarbonyl)-1,1-bis(triphenylarsine)palladacyclobutan-3-one, and 1,1-(2',2''-Bipyridyl)-2,4-bis(methoxycarbonyl)palladacyclobutan-3-one. *J. Chem. Soc. Dalton Trans.* **1985**, 259-268.

(23) Van Haaren, R. J.; Goubitz, K.; Fraanje, J.; van Strijdonck, G. P. F.; Oevering, H.; Coussens, B.; Reek, J. N. H.; Kamer, P. C. J.; van Leeuwen P. W. N. M. An X-ray Study of the Effect of the Bite Angle of Chelating Ligands on the Geometry of Palladium(allyl) Complexes: Implications for the Regioselectivity in the Allylic Alkylation. *Inorg. Chem.* **2001**, *40*, 3363-3372.

(24) Exchange at higher temperatures could not be monitored due to extensive complex decomposition.

(25) Becke, A. D. Density-functional thermochemistry. III. The role of exact exchange. *J. Chem. Phys.* **1993**, *98*, 5648-5652.

(26) Grimme, S.; Antony, J.; Ehrlich, S.; Krieg, H. A consistent and accurate *ab initio* parametrization of density functional dispersion correction DFT-D for the 94 elements H-Pu. *J. Chem. Phys.* **2010**, *132*, 154104.

(27) Gaussian 09, Revision D.01. Frisch, M. J.; Trucks, G. W.; Schlegel, H. B.; Scuseria, G. E.; Robb, M. A.; Cheeseman, J. R.; Scalmani, G.; Barone, V.; Mennucci, B.; Petersson, G. A.; Nakatsuji, H.; Caricato, M.; Li, X.; Hratchian, H. P.; Izmaylov, A. F.; Bloino, J.; Zheng, G.; Sonnenberg, J. L.; Hada, M.; Ehara, M.; Toyota, K.; Fukuda, R.; Hasegawa, J.; Ishida, M.; Nakajima, T.; Honda, Y.; Kitao, O.; Nakai, H.; Vreven, T.; Montgomery, Jr., J. A.; Peralta, J. E.; Ogliaro, F.; Bearpark, M.; Heyd, J. J.; Brothers, E.; Kudin, K. N.; Staroverov, V. N.; Keith, T.; Kobayashi, R.; Normand, J.; Raghavachari, K.; Rendell, A.; Burant, J. C.; Iyengar, S. S.; Tomasi, J.; Cossi, M.; Rega, N.; Millam, J. M.; Klene, M.; Knox, J. E.; Cross, J. B.; Bakken, V.; Adamo, C.; Jaramillo, J.; Gomperts, R.; Stratmann, R. E.; Yazyev, O.; Austin, A. J.; Cammi, R.; Pomelli, C.; Ochterski, J. W.; Martin, R. L.; Morokuma, K.; Zakrzewski, V. G.; Voth, G. A.; Salvador, P.; Dannenberg, J. J.; Dapprich, S.; Daniels, A. D.; Farkas, O.; Foresman, J. B.; Ortiz, J. V.; Cioslowski, J.; Fox, D. J. Gaussian, Inc., Wallingford CT, 2013.

(28) Francl, M. M.; Petro, W. J.; Hehre, W. J.; Binkley, J. S.; Gordon, M. S.; DeFrees, D. J.; Pople, J. A. Self-consistent molecular orbital methods. XXIII. A polarization-type basis set for second-row elements. *J. Chem. Phys.* **1982**, *77*, 3654-3665.

(29) Clark, T.; Chandrasekhar, J.; Schleyer, P. V. R. Efficient diffuse function-augmented basis sets for anion calculations. III. The 3-21+G

basis set for first-row elements, Li-F. *J. Comput. Chem.* **1983**, *4*, 294-301.

(30) Ehlers, A. W.; Böhme, M.; Dapprich, S.; Gobbi, A.; Höllwarth, A.; Jonas, V.; Köhler, K. F.; Stegmann, R.; Veldkamp, A.; Frenking, G. A set of f-polarization functions for pseudo-potential basis sets of the transition metals Sc-Cu, Y-Ag and La-Au. *Chem. Phys. Lett.* **1993**, *208*, 111-114.

(31) Roy, L. E.; Hay, P. J.; Martin, R. L. Revised Basis Sets for the LANL Effective Core Potentials. *J. Chem. Theory Comput.* **2008**, *4*, 1029-1031.